

Analogous Optical Activity in Free Space Using a Single Pancharatnam–Berry Phase Element

Sheng Liu,* Shuxia Qi, Peng Li, Bingyan Wei, Peng Chen, Wei Hu, Yi Zhang, Xuetao Gan, Peng Zhang, Yanqing Lu, Zhigang Chen,* and Jianlin Zhao*

It is commonly believed that optical activity (OA) is manifested mainly in chiral media, but rare in non-chiral structures. Here, an analog of OA in free space is experimentally demonstrated by using a single liquid-crystal Pancharatnam–Berry phase element (PBPE), for which the mechanism is highly consistent with that of the traditional OA. The specifically designed PBPE supports the direction-dependent polarization rotation of a Bessel beam with controllable “rotatory power.” Such a polarization rotation can be revoked by another PBPE with the same structure. Unlike in a chiral medium, this scheme shows simultaneous realization of equivalent levorotation and dextrorotation merely by switching the optical element orientation, promising for applications non-magnetic optical devices such as optical isolators.

1. Introduction

Optical activity (OA) commonly refers to the ability of an optical medium to rotate the polarization of light during propagation. It is now being extensively studied due to its important applications in analytical chemistry, biology, and crystallography. Traditionally, it was considered that OA occurs in natural media including chiral molecules. The chiral structures of molecular units, associated with the mirror asymmetry, are crucial in exhibiting the OA. Recently, several types of synthetic metamaterials with strong chirality have been constructed, exhibiting

broadband and nondispersive characteristics, or gigantic polarization rotatory power.^[1–5] In particular, it has been demonstrated that non-chiral metamaterials can also display OA, by introducing extrinsic chirality with oblique incidence,^[6,7] or by manipulating the phase difference between the two circularly polarized components.^[8]

In principle, OA is considered as a product of circular birefringence, relying much on the optically active materials. The circular birefringence is essentially a performance of extrinsic orbital angular momentum (OAM) variation affected by the spin states (circular polarizations), attributed to the spin–orbital interaction (SOI). The SOI of light has been extensively investigated for manifesting the spin-dependent variation^[9,10] through, for example, the spin Hall effect^[11–13] and spin-controlled shaping.^[14,15] One of the effective techniques to realize and even to enhance the SOI of light is to explore the Pancharatnam–Berry phase arising in polarization manipulations.^[15–20] An enhanced SOI enables a greater variation between the wave vectors of the two spin states, which guides the modulation of the extrinsic OAM. As such, OA is also artificially manifested by utilizing the SOI, for instance, by introducing topological Berry phase during trajectory variation^[21–24] in helical coiled optical fibers, or other twisted structures.^[25,26]

As neutral particles, photons can perform the SOI only by recourse to the media or structures. Until now, most of the reported OAs have been realized in specific materials, which have inherent constraints and limitations for many applications. There is no evidence that free space can support OA. However, in recent years, several ideas have been proposed to realize the polarization rotation or variation of light beams in free space, such as using radial-to-longitudinal mapping of axicon phase,^[27] superposing the modulated beams,^[28–30] manipulating the focal fields of metalens,^[31] and utilizing the nonlinear Gouy phase

S. Liu, S. Qi, P. Li, B. Wei, Y. Zhang, X. Gan, J. Zhao
Key Laboratory of Light-field Manipulation and Information Acquisition
Ministry of Industry and Information Technology, and Shaanxi Key
Laboratory of Optical Information Technology
School of Physical Science and Technology
Northwestern Polytechnical University
Xi'an 710129, China
E-mail: shengliu@nwpu.edu.cn; jlzhao@nwpu.edu.cn

P. Chen, W. Hu, Y. Lu
National Laboratory of Solid State Microstructures
Key Laboratory of Intelligent Optical Sensing and Manipulation
Collaborative Innovation Center of Advanced Microstructures, and
College of Engineering and Applied Sciences
Nanjing University
Nanjing 210093, China

P. Zhang
State Key Laboratory of Transient Optics and Photonics
Xi'an Institute of Optics and Precision Mechanics
Chinese Academy of Sciences
Xi'an 710119, China

Z. Chen
The MOE Key Laboratory of Weak-Light Nonlinear Photonics
TEDA Applied Physics Institute and School of Physics
Nankai University
Tianjin 300457, China
E-mail: zgchen@nankai.edu.cn

Z. Chen
Department of Physics and Astronomy
San Francisco State University
San Francisco, CA 94132, USA

 The ORCID identification number(s) for the author(s) of this article can be found under <https://doi.org/10.1002/lpor.202100291>

DOI: 10.1002/lpor.202100291

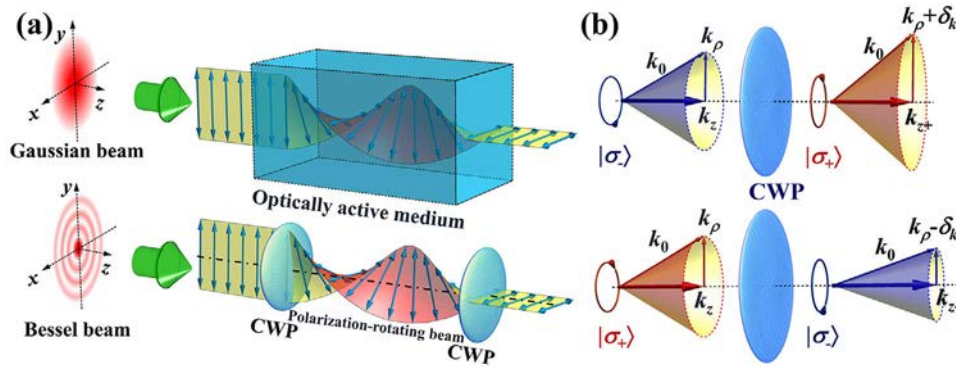


Figure 1. Schematic illustration of analogous optical activity (OA) of a Bessel beam in free space, as compared to that of a Gaussian beam in an active medium. a) Sketch of the traditional medium-based (top) and unusual free-space (bottom) OA, where the blue double-arrows denote the polarization orientations. b) Spin-orbital interaction of the Bessel beam triggered by a conical-wave plate (CWP), where $|\sigma_+\rangle$ and $|\sigma_-\rangle$ denote the spin states, the cones depict the spin-related change of wave vectors of Bessel beams.

difference.^[32] These proposed schemes bring about the possibilities to realize analogous OA in free space. However, the above work about free-space polarization rotation requires complicated optical setups, which hampers the controllability of OA analog and even limits the related applications.

In this work, we propose and demonstrate the analog of OA in free space by using a single liquid-crystal (LC) Pancharatnam-Berry phase element (PBPE), for which the mechanism of polarization rotation coincides well with the theory of circular birefringence. The PBPE is specifically designed to modulate an optical Bessel beam according to the spin-introduced wave vector bifurcation. After passing through the element, the linearly polarized Bessel beam exhibits direction-dependent polarization rotation during its subsequent propagation in free space. As such, it is transformed into a beam with equivalent OA which possesses the ability to rotate the polarization plane by itself. Comparing to the traditional OA in the active media, the analogous OA can remain intact in principle during subsequent free-space propagation, until it is unloaded by another PBPE (see Figure 1a). The optical rotatory power can be enhanced or reduced via specific optical elements placed at the input, or even after the polarization-rotating beam (PRB) is generated. Based on the direction-dependent polarization rotation, we also discuss the scheme for production of nonmagnetic optical components resembling polarization rotators, isolators, and circulators. Our scheme could be adopted for realization of medium-free OA with other transverse waves ranging from radio to optical frequencies.

2. Results and Discussion

2.1. Analogous Theory of Optical Activity

To resemble the circular birefringence of light in free space, we first need a solution to adjust the velocity of the spin states. It is easy to associate with a plane wave with a tilted wave vector, of which the phase velocity is determined by the axial component of the wave vector.^[32] While for a symmetric system, the wave with a conical wave vector, for example, a Bessel beam, is preferred, of which the velocity can be varied by manipulating the wave vector cone. A light wave with a Bessel profile $J_0(k_\rho \rho)$ (or with a conical phase $\exp(ik_\rho \rho)$, equivalently) can be considered as a superposi-

tion of a series of plane waves with wave vectors all located on a cone with a radius k_ρ (see Section S2, Supporting Information). The dynamic phase delay of the Bessel beam along the propagation axis is determined by the wave vector components k_z , which directly decides the phase velocity. Such a relation is expressed as

$$\varphi_z(k_\rho) = k_z z = \sqrt{k_0^2 - k_\rho^2} z \quad (1)$$

where $k_0 = 2\pi/\lambda$ is the wave vector. This is also consistent with the theory of Gouy phase shift.^[33] From the above equation, it can be concluded that a spin-dependent change of k_ρ would lead to the bifurcation of φ_z for different circular polarizations.

The spin-dependent change of wave vector could be realized by the Pancharatnam-Berry phase, which is a phase shift acquired by an optical wave during the polarization transformation. Based on the theory of Pancharatnam-Berry phase, different PBPEs have been proposed to control the wavefront and polarization state,^[15,17,19,34,35] to enhance the SOI,^[16] and even to exploit applications such as measurement of rotational speed^[18,36] and super-resolution image.^[20] Here, we introduce a specially designed PBPE—the conical-wave plate (CWP, see Section S1, Supporting information). This element can be considered as a half-wave plate with its local fast axes arranged conically, that is, $\Theta = -\delta_k \rho / 2$, where δ_k is a constant describing the varying frequency along radial coordinate ρ . The CWP can mediate the exchange between the spin and orbital parts of the angular momentum of light by inducing the spin-related geometric phase. It reverses the spins and attaches different Pancharatnam-Berry phases to them. For instance, the right- ($|\sigma_+\rangle$) and left-handed ($|\sigma_-\rangle$) spin states are transformed into left- and right-handed ones ($|\sigma_-\rangle$ and $|\sigma_+\rangle$), with appended phases $\exp(\pm i\delta_k \rho)$, respectively (see Section S1.3 Supporting information for details). Thus, the corresponding conical wave vectors are changed to $k_\rho \pm \delta_k$. The wave vector cones for left- and right-handed spins expand and contract, respectively, with their slant heights keeping a constant k_0 , as shown in Figure 1b. From another perspective, this is a manifestation of photonic SOI induced by the CWP. It is widely known that the OAM of light consists of the intrinsic and extrinsic parts, which are relative to the center of the light beam (independent on the axis location, e.g., vortex beam) and a

chosen spatial axis (describing the motion of photons), respectively. The spin-dependent bifurcation of wave vector changes the local motions of the spin states, representing a typical spin-related transformation of local extrinsic OAM. Namely, a change of the spin angular momentum will modify the extrinsic OAM of light.

Therefore, the two circularly polarized components of the Bessel beam acquire a z -dependent difference of dynamic phase delays

$$\epsilon\varphi_z = \varphi_z(k_+) - \varphi_z(k_-) = -4k_\rho\delta_k z / \left(\sqrt{k_0^2 - k_+^2} + \sqrt{k_0^2 - k_-^2} \right) \quad (2)$$

where $k_\pm = k_\rho \pm \delta_k$. Under the paraxial condition, this phase difference exhibits a nearly linear variation with propagation distance if δ_k is small enough, revealing the circular birefringence of light exhibited in free space.

For a monochromatic zero-order Bessel beam with linear polarization propagating along z -axis, the complex amplitude is described by $\mathbf{E}_{\text{in}} = J_0(k_\rho\rho)|\mathbf{L}(\theta_0)\rangle$, where $|\mathbf{L}(\theta_0)\rangle = [\cos\theta_0, \sin\theta_0]^T$ denotes the linear polarization along angle θ_0 . When it enters to the CWP, the resulting field presents polarization rotation due to the circular birefringence as schematically shown in Figure 1a. In the near-axis region, and under the approximation condition $\delta_k \ll k_\rho \ll k_0$, it can be expressed as (see details in Section S2.3, Supporting information)

$$|\mathbf{E}_{\text{out}} \approx J_0(k_\rho\rho) \left| \mathbf{L} \left(\frac{k_\rho\delta_k}{k_0} z - \theta_0 \right) \right. \quad (3)$$

This key relation indicates that a rotating polarization is introduced for subsequent propagation to the otherwise linearly polarized Bessel beam by the CWP. It has striking similarities with the traditional OA: 1) Linear rotation: the rotation angle of polarization direction is proportional to the propagation distance. Here, we introduce and define a term “the specific rotation (SR)” as the rotation angle in unit propagation length, that is, $[\alpha] = k_\rho\delta_k/k_0$, to characterize the quantitative rotation. 2) Circular birefringence: the SR is proportional to the radial frequency of the CWP δ_k , which can be viewed as a description of the amount of circular birefringence for the medium. 3) Optical rotatory “dispersion”: the SR is proportional to the wave vector k_ρ of the Bessel beam which decides the phase velocity, representing the response difference of the CWP with respect to different spatial spectrum. 4) Non-reciprocal-like propagation (see Figure 3: unlike in an optically active medium, different launching directions of a beam to the same CWP result in opposite polarization rotations, that is, optical dextrorotation and levorotation).

2.2. Polarization-Rotating Beam

The above analogous OA can be considered as an intrinsic nature of this type of Bessel beam. Once such a beam exits the CWP, the wave packet will never be restrained in free space, and its subsequent evolution just depends on its internal parameters such as complex amplitude and polarization. In other words, this beam itself has the optical rotatory power, and can be termed as a PRB.

Under ideal condition, a stable PRB is expressed by the interference of two Bessel spin states with different radial wave vectors, written as

$$|\mathbf{E}_{\text{PRB}} = \vartheta_0 \mathbf{T} \left(-\frac{\epsilon\varphi_z}{2} \right) \begin{bmatrix} \cos\sqrt{\cdot} \\ i \sin\sqrt{\cdot} \end{bmatrix} \quad (4)$$

where $\vartheta_0 = \sqrt{J_0(k_+\rho)^2 + J_0(k_-\rho)^2}/2$, $\Theta = \arctan[J_0(k_-\rho)/J_0(k_+\rho)] - \pi/4$, $\mathbf{T}(-\Delta\varphi_z/2)$ is a matrix denoting an anticlockwise rotation operation with rotation angle $\Delta\varphi_z/2$ (see Equation (S9), Supporting Information). Obviously, the polarization of the PRB is not exactly a uniform linear one. It has the hybrid elliptical polarization with radially varied ellipticity ($\tan\Theta$) and same orientation ($\Delta\varphi_z/2$) in a transverse plane, due to the mismatching between the left- and right-handed polarized components (see Figure 2a). The purity of linear polarization along $\Delta\varphi_z/2$ is related to the value of δ_k ($\approx 91\%$ for 7 central rings when $\delta_k = k_\rho/20$). The polarization orientation integrally rotates with propagation distance, as also shown in Figure 2b and the polarization rotation direction is determined by the sign of δ_k (see Equation (2)). It should be noted that, even though the non-uniform polarization mainly dominates the free-space polarization rotation, it needs to match the Bessel profile indispensably to introduce the difference of dynamic phase.

More importantly, due to the Bessel profile, the PRB also exhibits the non-diffraction and self-healing properties during propagation as does the Bessel beam. The non-diffraction property provides a perfect model that the only variable is the z -dependent phase difference between the two spin states (see Equation (S5), Supporting Information). Hence, the PRB can be considered as a solution of Helmholtz equation, which possesses the z -invariant complex amplitude and the linearly rotated polarization along z -axis in theory. The self-healing property guarantees the stability of SR of the PRB. Figure 2c shows the calculated rotating angle of polarization of the main lobe versus propagation distance for the PRB with and without a blocker. It reveals that the PRB can preserve its linear rotation after a certain distance of propagation even when it is blocked partially.

2.3. Experimental Demonstration

To experimentally demonstrate the free-space polarization rotation, a collimated laser beam (He-Ne laser, 632.8 nm) is transformed into a Bessel mode via an axicon (Ax) lens, and then passes through the CWP ($\delta_k = \pi \text{ mm}^{-1}$) made of LC, as shown in Figure 3a. Considering that the non-diffracting distance of the axicon is finite, the CWP is put close to the axicon to guarantee a long effective distance as much as possible for observing the polarization rotation. To monitor the dynamical propagation of the PRB, the intensity distribution of the output beam is recorded by a CCD camera moved along the propagation direction step by step. Figure 3b shows the propagation process of the beam to a distance of 16 cm, which is displayed by the 3D intensity distribution of the recorded beam profiles. It exhibits a non-diffraction Bessel profile. When this propagation process is analyzed by an analyzer P_2 , the resulting Bessel beam undergoes a periodic variation in intensity. Figure 3c shows the intensity variation along propagation direction after passing the horizontal (top) and vertical (bottom) analyzers, which describe the horizontally

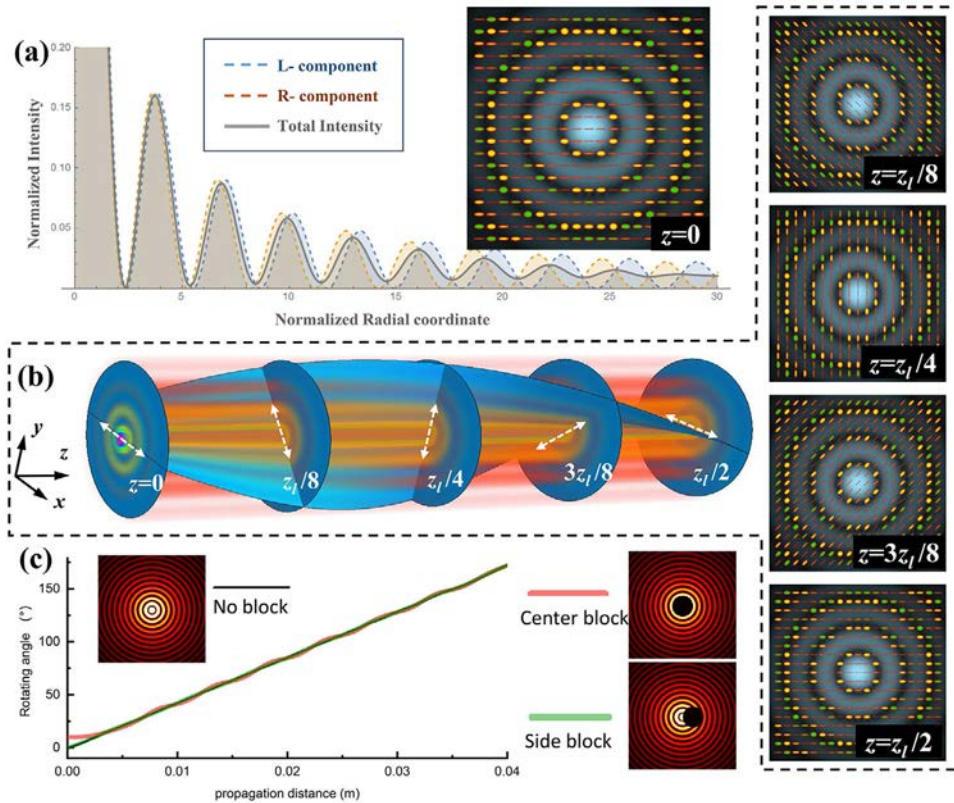


Figure 2. Properties of polarization-rotating beam (PRB). a) Amplitudes profiles of the PRB and its left- and right-handed polarized components (L- and R-components). Inset: the amplitude (background) and polarization (ellipses) distributions of the PRB, where yellow and green ellipses denote right- and left-handed polarization, respectively. b) Polarization rotation of the PRB during propagation within half period of rotation ($z_1/2$). White arrowheads denote the polarization orientation. c) Rotating angle versus propagation distance for the PRBs with and without a blocker.

(E_x) and vertically (E_y) polarized components of the light beam, respectively. The anti-phase intensity extinction in these two pictures reveals clearly the polarization rotation associated with the PRB.

To measure the rotation angle precisely, we increase the exposure of the CCD to obtain an over-saturated picture, and rotate the analyzer P_2 to detect the angle for extinction perpendicular to the polarization angle. The rotation angle versus propagation distance is shown as the yellow circles in Figure 3e changing in a perfectly linear fashion. The pink solid line in Figure 3e shows the data fitting, where the slope $[\alpha]$ is measured to be $1.117^\circ \text{ mm}^{-1}$, coinciding well with the theoretical prediction (see Section S3, Supporting information). It is noted that this rotation is comparable to that in bulk materials such as quartz crystals or sucrose solutions, although nowadays giant OA can be achieved in engineered planar metasurfaces.^[1]

Conventional optically active materials show reciprocity for which dextrorotation or levorotation of a light beam is independent of the propagation direction, unless the reciprocity is broken as with the Faraday effect. Interestingly, the proposed CWP provides an opportunity to induce the magnetic-free direction-dependent polarization rotation (see Figure 3d), since the rotation of polarization plane closely depends on the direction of propagation. From the view of the front and back sides of the CWP, the axis orientations are $-\delta_k \rho/2$ and $\delta_k \rho/2$, respectively. It means that the sign of the radial frequency is reversed when

changing the input direction, and, consequently, so is the SR $[\alpha]$. To experimentally verify this direction-dependent polarization rotation, the CWP is flipped to change the input direction of the Bessel beam. The measured rotation angle versus propagation distance behaves a reverse trend of linear variation in comparison (Figure 3e) with the case before flipping the CWP. The SR is measured to be $[\alpha] = -1.103^\circ \text{ mm}^{-1}$, showing dextrorotation.

It is notable that in Figure 3e the polarization rotation shows a perfect linear trend within 16 cm. However, the distance for polarization rotation is mainly determined by the non-diffraction distance of the input Bessel beam ($\approx 20 \text{ cm}$ in this experiment), which could be made much longer by proper initial truncation. In addition, the measured SRs for levorotation and dextrorotation are both slightly different from the theoretical value $1.19^\circ \text{ mm}^{-1}$. This discrepancy might be caused by the process error of CWP, the measuring error of rotation angle, and even by the beam quality and alignment. If only comparing the measured SRs, the relative uncertainty is acceptable ($\approx 1.2\%$).

2.4. Control of Specific Rotation

There are two key parameters deciding the appearance of the PRB: the radial wave vector k_ρ of input Bessel beam and the radial frequency δ_k of the CWP, mainly determining the complex

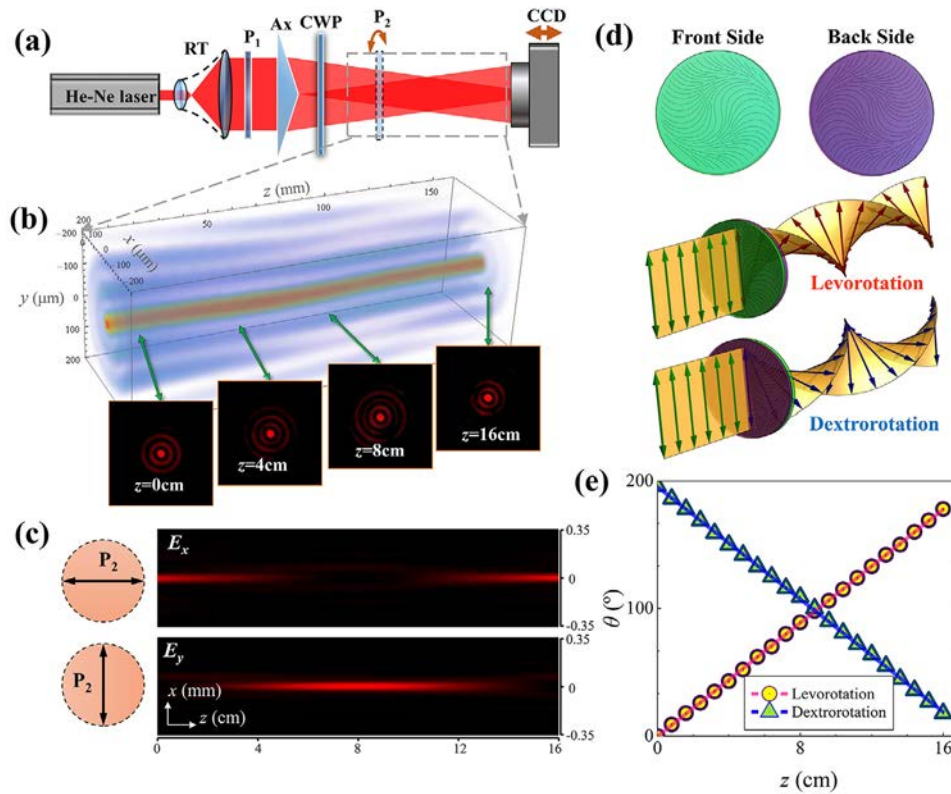


Figure 3. Experimental demonstration of direction-dependent analogous OA in free space. a) Experimental setup. b) Non-diffraction propagation of a Bessel beam captured by CCD. c) Side-view of x- (top) and y-polarized (bottom) components of the beam corresponding to b). d) Schematic of the levorotation and dextrorotation obtained with opposite inputs to the CWP. e) Measured polarization angle versus propagation distance for the two cases.

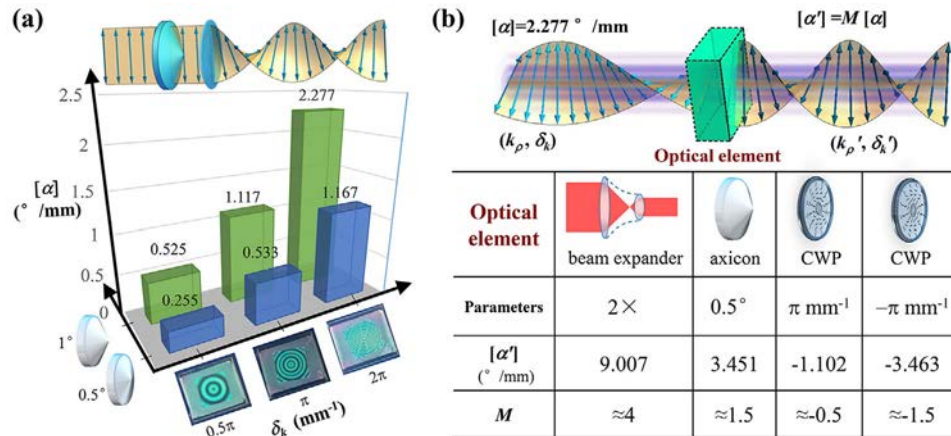


Figure 4. Control of the rotatory power of PRB. a) Measured specific rotation (SR) of the PRB with different δ_k and k_ρ . b) Schematic of the magnification of SR via an optical element (top) and the list of measured SR $[\alpha']$ and magnification M (bottom table); A minus M means the opposite rotation of polarization.

amplitude and polarization profiles, respectively. The optical rotatory power of the PRB (rested with the SR $[\alpha]$) also depends linearly on k_ρ and δ_k . Here, we employ another axicon (with physical angle 0.5°) and other two CWPs ($\delta_k=2\pi$ and $0.5\pi \text{ mm}^{-1}$) to generate the PRB with different rotatory powers. According to the linear variation of polarization angle with distance, we can quickly measure the SR by recording the rotation angle in

a certain distance. **Figure 4a** depicts the measured SR versus k_ρ and δ_k , supporting the expected conclusion above.

Interestingly, the rotatory power is also tunable even after the PRB is already formed, by employing a special optical element (see **Figure 4b**), such as a beam expander, an axicon, or the CWP. When a PRB with $[\alpha]=2.277^\circ \text{ mm}^{-1}$ (generated by axicon of 1° and CWP with $\delta_k=2\pi \text{ mm}^{-1}$) passes through a reversed $2\times$

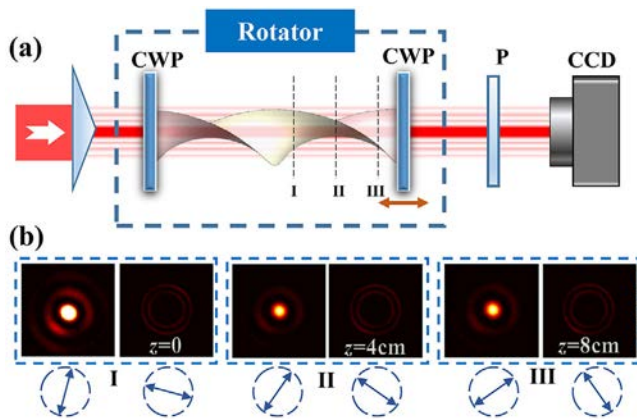


Figure 5. An example of proposed application of the PRB. a) Schematic of a polarization rotator consisting of a pair of CWPs. b) Output intensities of the beam passing through the rotatable analyzer P for the second CWP moved to the positions I, II, and III, where the double-arrows denote the analyzer orientation.

beam expander, the measured SR is $9.007^\circ \text{ mm}^{-1}$, increasing up to ≈ 4 times. It means that the SR can be magnified with micrographics. When an additional axicon or CWP is inserted, the parameter k_p or δ_k is modified, and thus the SR is changed. The magnification M of $[\alpha]$ equals to the product of the magnifications of k_p and δ_k (see Section S4, Supporting information).

2.5. Polarization Rotator

The most widely used device based on non-reciprocal OA is the Faraday rotator—the key component of optical isolators and circulators. We illustrate here above demonstrated free-space polarization rotation also has the capacity to form a polarization rotator owing to its direction-dependent property. The challenge is that the polarization of the PRB tends to be rotated without stopping during propagation because of the intrinsic polarization rotating feature of the beam. To unload the polarization rotation, another CWP identical to the one used to generate the PRB has been employed to slow down and eventually stop the polarization rotation, as shown in Figure 5a. Movie S1 (Supporting Information) clearly demonstrates the comparison between the dynamic evolutions of the PRB passing through an analyzer before and after its rotating feature is unloaded. From the analyzed images, it experimentally verifies that the PRB is reduced to a linearly polarized Bessel beam, which no longer rotates. The output polarization orientation can be controlled by the distance between the two CWPs. Figure 5b shows the analyzed results by moving the second CWP, and reveals the controllable output polarization. The pair of CWP forms a typical direction-dependent polarization rotator for the Bessel beam: inputting from different sides leads to polarization rotation in different directions. By adjusting the output polarization along 45° , we can construct an isolator and a circulator as illustrated in Figure S4, Supporting Information. The isolator is formed by inserting two polarizers with axis along 90° and 45° before and after the rotator, respectively. The vertically polarized input beam obtains a polarization rotation of 45° through the rotator, while the back-propagating beam encounters an additional 45° rotation, and is isolated by the front polarizer (see

Figure S4a, Supporting Information). The insertion loss and isolation of this system are measured to be ≈ 2.08 and ≈ 13.3 dB, respectively. The high losses mainly come from the transformation between the transmission modes. Besides, since the polarization rotation is realized by the PBPE, it is only for monochromatic light. The change of the working wavelength would lead a complicated polarization transformation. Thus, the isolator could hardly be applicable for the broadband incident light. Although the performance indices of the proposed isolator are not comparable to those of the commercially available ones, it offers a possibility for exploring novel applications based on non-reciprocal-like polarization rotation without media.

2.6. Discussion

We point out that, in order to generate the proposed PRBs, one needs to carefully match the centers of the input beam, axicon, and CWP, but only the axicon and CWP need to be aligned. The shift of input beam just reduces the purity of linear polarization without affecting the polarization rotation much. As to other input beams with circular symmetry, such as a vortex beam or a cylindrical vector beam, the free-space polarization rotation would also happen, and the polarizations integrally rotate. Furthermore, higher-order Bessel beams and vector Bessel beams can also be formed after going through the axicon, which would have the same wave vector cone as that of the zero-order one, with the same SR discussed above.

3. Conclusion

In conclusion, we have demonstrated a method to endow a light beam with polarization rotating feature by utilizing SOI of light with a CWP, leading to polarization rotation in free space without requiring any active media or specially designed materials. OA phenomenon leads to direction-dependent propagation of light as its polarization rotation depends on the propagation direction. The polarization rotating feature of the beam can be selectively switched on or off by another CWP, which supports the realization of direction-dependent polarization rotators. Our work brings about the possibilities to develop medium-free non-reciprocal-like photonic devices such as optical isolators and circulators.

Supporting Information

Supporting Information is available from the Wiley Online Library or from the author.

Acknowledgements

This research was supported by the National Key R&D Program of China (2017YFA0303800), the National Natural Science Foundations of China (NSFC) (11634010, 12074312, 61675168, 12074313, 11774289, 91850118, 11804277, and 11574389), Basic Research Plan of Natural Science in Shaanxi province (2019JM-583), and Fundamental Research Funds for the Central Universities (3102019JC008), Innovation Foundation for Doctor Dissertation of Northwestern Polytechnical University (CX202047).

Conflict of Interest

The authors declare no conflict of interest.

Data Availability Statement

The data that support the findings of this study are available from the corresponding author upon reasonable request.

Keywords

Bessel beams, liquid crystal, Pancharatnam–Berry phase, polarization rotation

Received: May 31, 2021

Revised: September 14, 2021

Published online: November 13, 2021

-
- [1] A. Y. Zhu, W. T. Chen, A. Zaidi, Y.-W. Huang, M. Khorasaninejad, V. Sanjeev, C.-W. Qiu, F. Capasso, *Light: Sci. Appl.* **2018**, *7*, 17158.
- [2] H. S. Park, T.-T. Kim, H.-D. Kim, K. Kim, B. Min, *Nat. Commun.* **2014**, *5*, 5435.
- [3] M. Kuwata-Gonokami, N. Saito, Y. Ino, M. Kauranen, K. Jefimovs, T. Vallius, J. Turunen, Y. Svirko, *Phys. Rev. Lett.* **2005**, *95*, 227401.
- [4] A. Papakostas, A. Potts, D. M. Bagnall, S. L. Prosvirnin, H. J. Coles, N. I. Zheludev, *Phys. Rev. Lett.* **2003**, *90*, 107404.
- [5] A. V. Rogacheva, V. A. Fedotov, A. S. Schwanecke, N. I. Zheludev, *Phys. Rev. Lett.* **2006**, *97*, 177401.
- [6] M. Ren, E. Plum, J. Xu, N. I. Zheludev, *Nat. Commun.* **2012**, *3*, 833.
- [7] E. Plum, X. Liu, V. A. Fedotov, Y. Chen, D. P. Tsai, N. I. Zheludev, *Phys. Rev. Lett.* **2009**, *102*, 113902.
- [8] P. Yu, J. Li, C. Tang, H. Cheng, Z. Liu, Z. Li, Z. Liu, C. Gu, J. Li, S. Chen, J. Tian, *Light: Sci. Appl.* **2016**, *5*, e16096.
- [9] F. Cardano, L. Marrucci, *Nature Photon.* **2015**, *9*, 776.
- [10] K. Y. Bliokh, F. J. Rodríguez-Fortuño, F. Nori, A. V. Zayats, *Nature Photon.* **2015**, *9*, 796.
- [11] O. Hosten, P. Kwiat, *Science* **2008**, *319*, 787.
- [12] K. Y. Bliokh, Y. P. Bliokh, *Phys. Rev. Lett.* **2006**, *96*, 073903.
- [13] M. Onoda, S. Murakami, N. Nagaosa, *Phys. Rev. Lett.* **2004**, *93*, 083901.
- [14] L. Marrucci, C. Manzo, D. Paparo, *Phys. Rev. Lett.* **2006**, *96*, 163905.
- [15] D. Lin, P. Fan, E. Hasman, M. L. Brongersma, *Science* **2014**, *345*, 298.
- [16] X. Yin, Z. Ye, J. Rho, Y. Wang, X. Zhang, *Science* **2013**, *339*, 1405.
- [17] E. Karimi, S. A. Schulz, I. De Leon, H. Qassim, J. Upham, R. W. Boyd, *Light Sci. Appl.* **2014**, *3*, e167.
- [18] D. Hakobyan, E. Brasselet, *Nature Photon.* **2014**, *8*, 610.
- [19] A. Arbabi, Y. Horie, M. Bagheri, A. Faraon, *Nat. Nanotechnol.* **2015**, *10*, 937.
- [20] M. Khorasaninejad, W. T. Chen, R. C. Devlin, J. Oh, A. Y. Zhu, F. Capasso, *Science* **2016**, *352*, 1190.
- [21] M. V. Berry, *Nature* **1987**, *326*, 277.
- [22] A. Tomita, R. Y. Chiao, *Phys. Rev. Lett.* **1986**, *57*, 937.
- [23] R. Y. Chiao, Y. S. Wu, *Phys. Rev. Lett.* **1986**, *57*, 933.
- [24] K. Y. Bliokh, A. Niv, V. Kleiner, E. Hasman, *Nature Photon.* **2008**, *2*, 748.
- [25] Z. H. Jiang, L. Kang, D. H. Werner, *Nat. Commun.* **2017**, *8*, 356.
- [26] X. M. Xi, T. Weiss, G. K. L. Wong, F. Biancalana, S. M. Barnett, M. J. Padgett, P. St J Russell, *Phys. Rev. Lett.* **2013**, *110*, 143903.
- [27] I. Moreno, J. A. Davis, M. M. Sánchez-López, K. Badham, D. M. Cottrill, *Opt. Lett.* **2015**, *40*, 5451.
- [28] J.-Q. Lü, X.-L. Wang, G.-L. Zhang, C. Tu, Y. Li, H.-T. Wang, *Opt. Lett.* **2020**, *45*, 1738.
- [29] A. H. Dorrah, N. A. Rubin, A. Zaidi, M. Tamagnone, F. Capasso, *Nature Photon.* **2021**, *15*, 287.
- [30] P. Li, D. Wu, Y. Zhang, S. Liu, Y. Li, S. Qi, J. Zhao, *Photon. Res.* **2018**, *6*, 756.
- [31] X. Fan, P. Li, X. Guo, B. Li, Y. Li, S. Liu, Y. Zhang, J. Zhao, *Phys. Rev. Applied* **2020**, *14*, 024035.
- [32] D. Giovannini, J. Romero, V. Potoček, G. Ferenczi, F. Speirits, S. M. Barnett, D. Faccio, M. J. Padgett, *Science* **2015**, *347*, 857.
- [33] P. Martelli, M. Tacca, A. Gatto, G. Moneta, M. Martinelli, *Opt. Express* **2010**, *18*, 7108.
- [34] L. Huang, X. Chen, H. Mühlenbernd, G. Li, B. Bai, Q. Tan, G. Jin, T. Zentgraf, S. Zhang, *Nano Lett.* **2012**, *12*, 5750.
- [35] Z. Bomzon, G. Biener, V. Kleiner, E. Hasman, *Opt. Lett.* **2002**, *27*, 1141.
- [36] F. Yue, A. Aadhi, R. Piccoli, V. Aglieri, R. Macaluso, A. Toma, R. Morandotti, L. Razzari, *Laser Photonics Rev.* **2021**, *15*, 2000576.